The dimeric structure of the cytochrome bc(1) complex prevents center P inhibition by reverse reactions at center N. Biochim Biophys Acta

ARTICLE *in* BIOCHIMICA ET BIOPHYSICA ACTA · JULY 2008

Impact Factor: 4.66 · DOI: 10.1016/j.bbabio.2008.04.008 · Source: PubMed

2 AUTHORS, INCLUDING:

Raul Covian
U.S. Department of Health and Human Services
32 PUBLICATIONS **602** CITATIONS

Published in final edited form as:
Biochim Biophys Acta. 2008 ; 1777(7-8): 1044–1052.

The dimeric structure of the cytochrome bc_1 complex prevents center P inhibition by reverse reactions at center N

Raul Covian and **Bernard L. Trumpower**[a]
Department of Biochemistry, Dartmouth Medical School, Hanover, New Hampshire 03755, U.S.A.

Summary

Energy transduction in the cytochrome bc_1 complex is achieved by catalyzing opposite oxido-reduction reactions at two different quinone binding sites. We have determined the pre-steady state kinetics of cytochrome *b* and c_1 reduction at varying quinol/quinone ratios in the isolated yeast bc_1 complex to investigate the mechanisms that minimize inhibition of quinol oxidation at center P by reduction of the b_H heme through center N. The faster rate of initial cytochrome *b* reduction as well as its lower sensitivity to quinone concentrations with respect to cytochrome c_1 reduction indicated that the b_H hemes equilibrated with the quinone pool through center N before significant catalysis at center P occurred. The extent of this initial cytochrome *b* reduction corresponded to a level of b_H heme reduction of 33%–55% depending on the quinol/quinone ratio. The extent of initial cytochrome c_1 reduction remained constant as long as the fast electron equilibration through center N reduced no more than 50% of the b_H hemes. Using kinetic modeling, the resilience of center P catalysis to inhibition caused by partial pre-reduction of the b_H hemes was explained using kinetic in terms of the dimeric structure of the bc_1 complex which allows electrons to equilibrate between monomers.

Keywords

bc_1 complex; Electron transfer; Quinone; Semiquinone

1. Introduction

The cytochrome bc_1 complex is a multi-subunit dimer [1–5] that converts the energy derived from quinol oxidation into the movement of electrical charges across the membrane in which it is embedded by catalyzing opposite reactions at its two quinone binding sites. As explained by the protonmotive Q cycle mechanism, [6,7], one of the two electrons coming from the oxidation of quinol at center P is transferred to cytochrome *c* via the Rieske protein and cytochrome c_1. The other electron from quinol moves from the b_L to the b_H heme towards the negative side of the membrane dielectric and reduces quinone bound at center N to form a tightly bound semiquinone [8–10]. Alternatively, this stable semiquinone can be formed by the direct one-electron oxidation of quinol at center N with the accompanying reduction of the b_H heme. This reaction is readily observable when center P is blocked by inhibitors and quinol is added [11–15], but is also expected to occur to some extent under uninhibited conditions

a To whom correspondence should be addressed: Department of Biochemistry, Dartmouth Medical School, 7200 Vail, Hanover, NH 03755. Phone: 603-650-1621; Fax: 603-650-1128; E-mail: Trumpower@Dartmouth.edu.

given the full reversibility of the Q cycle mechanism [16], especially when quinol is present at higher concentrations than quinone.

If significant reduction of the b_H heme through center N occurs, catalysis at center P would be inhibited because of the lower equilibrium constant for quinol oxidation when only the b_L heme is available to accept the second electron from the substrate [17]. This in turn would favor detrimental side reactions, such as the one electron reduction of oxygen to form superoxide [18]. Therefore, mechanisms that avoid the excessive accumulation of electrons in cytochrome *b* by quinol oxidation at center N are expected to exist. We have recently proposed that electron equilibration between the b_L hemes in the dimer, together with a preferential binding of quinol and quinone to center N depending on the redox state of the b_H heme, favor the oxidation of cytochrome *b* [15]. However, these studies were performed in the presence of center P inhibitors to isolate center N, so the effectiveness of the proposed mechanisms in favoring center P catalysis was not evaluated. Previous studies have reported the pre-steady state kinetics in the uninhibited enzyme, but have interpreted the reduction of cytochrome *b* as a result of quinol oxidation at center P [11,12,19,20].

In the present work, we have analyzed the simultaneous reduction of cytochrome *b* and c_1 at different quinol/quinone ratios in the isolated yeast enzyme in the absence of inhibitors. Our results indicate that the b_H hemes equilibrate rapidly with quinol and quinone through center N, and that center P catalysis is mostly insensitive to this partial pre-reduction of the b_H hemes. We discuss how electron transfer between the cytochrome *b* subunits of the dimer minimizes the potential inhibition of quinol oxidation at center P by the reduction of the b_H hemes through center N.

2. Materials and methods

2.1 Materials

Dodecylmaltoside was obtained from Anatrace. DEAE Bio-Gel A was obtained from Bio-Rad laboratories. Decyl-ubiquinone, Tween-20, diisopropyl fluorophosphate, sodium ascorbate and sodium dithionite were purchased from Sigma Chemical Co. Decyl-ubiquinol was prepared from decyl-ubiquinone as described previously [21]. These two compounds were quantified by UV spectroscopy using extinction coefficients of 16.0 mM^{-1} cm^{-1} for decyl-ubiquinone and 4.14 mM^{-1} cm^{-1} for decyl-ubiquinol [22].

2.2 Purification of cytochrome bc_1 complex

Wild-type bc_1 complex was isolated from commercially available Red Star bakerys yeast by anionic-exchange chromatography as described previously [23]. Quantification of the bc_1 complex was performed as reported before [24], using extinction coefficients of 17.5 mM^{-1} cm^{-1} for cytochrome c_1 [25] and 25.6 mM^{-1} cm^{-1} for the average absorbance of the b_L and b_H heme in cytochrome *b* [26]. The b_H heme in each monomer was considered to have an extinction coefficient of 36 mM^{-1} cm^{-1}, considering that it contributes to ~70% of the total cytochrome *b* absorbance [27]. The amount of endogenous ubiquinone copurified with the bc_1 complex was determined as described before [13] and determined to be 0.9 ± 0.1 molecules/bc_1 monomer. The purified enzyme was in the fully oxidized form as verified by the lack of spectral change upon addition of ferricyanide.

2.3 Pre-steady state reduction of bc_1 complex

Reduction of the cytochrome bc_1 complex was followed at room temperature (23 °C) by stopped flow rapid scanning spectroscopy using the OLIS Rapid Scanning Monochromator as previously reported [24]. Reactions were started by rapid mixing of 2 μM isolated enzyme in assay buffer containing 50 mM phosphate (pH 7.0), 1 mM sodium azide, 0.2 mM EDTA, 0.05%

Tween-20 and varying concentrations of decyl-ubiquinone against an equal volume of the same buffer containing varying concentrations of decyl-ubiquinol. The concentration of decyl-ubiquinol diluted in this buffer remained constant for at least tens of minutes as verified by UV-spectroscopy (not shown), excluding the possibility of auto-oxidation. No reduction of c_1 or b_H hemes in the presence of both antimycin and stigmatellin was detectable during the time scale of the assays, indicating that non-enzymatic reaction of decyl-ubiquinol with these redox centers was negligible. For each experiment, eight to ten data sets were averaged after subtracting the oxidized spectrum. The time course of absorbance change at 539, 554, 562, and 578 nm was extracted using software from OLIS and exported to the Origin 5.0 (OriginLab Corp.) program. The difference in absorbance between 554 and 539 nm (cytochrome c_1) and 562–578 nm (cytochrome *b*) was plotted and fitted to a second or third order exponential equation that included a lag phase to obtain rates and extents of reduction for each kinetic phase.

2.4 Kinetic modeling of electron equilibration at center N

The DynaFit program (BioKin, Ltd.), which allows simulation of reaction mechanisms described as a series of individual reaction steps [28], was used to estimate the relative concentration of the different species of dimers or monomers with semiquinone at center N and/or reduced or oxidized b_H heme. Two models (Fig. 1) were used in the simulations of electron equilibration through center N at different quinol/quinone ratios. The dimeric model considered the bc_1 complex as a functional dimer (E) in which electrons are able to move from one b_H heme to the other through the b_L hemes [13], whereas the monomeric model assumed that electrons can only enter and exit through one center N. Both models considered semiquinone to be a tightly bound ligand, and the binding of quinol and quinone to a particular center N was assumed to occur only when the b_H heme was oxidized or reduced, respectively. The enzyme monomer concentration was assumed to be 1 μM, and the sum of quinol and quinone was assumed to be 31 μM. The equilibrium constant for quinol binding was fixed to 45 μM based on the K_m value obtained for cytochrome *b* reduction, and expressed as association (k_{aQH}) and dissociation (k_{dQH}) constants with arbitrary values of 2 $\mu M^{-1}\ s^{-1}$ and 90 s^{-1}, respectively. Quinone binding and dissociation was expressed as rate constants (k_{aQ} and k_{dQ}) with identical to those used for quinol.

Equilibrium constants for the formation of semiquinone (SQ) were calculated assuming midpoint redox potentials (E_{m7}) of 80 mV for the b_H heme [27], 40 mV for the quinol/semiquinone couple [15], and 162 mV for the semiquinone/quinone couple [15]. Applying the Nernst equation as described previously [13], a ratio of rate constants of 2.18 and 4.97 were used, respectively, to simulate the formation of semiquinone from quinol and quinone. These ratios were expressed by fixing the reverse rates for both semiquinone forming reactions (k_{-1} and k_2 in Fig. 1) to an arbitrary value of $10^4\ s^{-1}$, resulting in forward rates of $k_1 = 2.18 \times 10^4\ s^{-1}$ and $k_{-2} = 4.97 \times 10^4\ s^{-1}$. In the case of the dimeric model, the rate of intermonomeric electron equilibration was fixed to a value of $k_{IM} = 300\ s^{-1}$ based on the rates of electron tunneling between the b_L and b_H hemes and between the b_L hemes, calculated as follows. For the yeast dimer, the edge-to-edge distance between the b_L hemes is 13.8 Å, whereas 12.4 Å separate the b_L and b_H hemes in each monomer [4]. According to the simplified equation for the calculation of electron transfer rates when redox centers have the same potential [29], a distance of 13.8 Å would allow a tunneling rate of $3.27 \times 10^4\ s^{-1}$. The calculated rate of b_L to b_H electron tunneling for yeast can be estimated to be $\sim 1.3 \times 10^6\ s^{-1}$ based on the equation for calculating an exergonic electron transfer [29]. If this same equation is used to calculate the rate of the reverse electron tunneling event, as has recently been proposed [30], the b_H to b_L transfer rate would be $3.2 \times 10^4\ s^{-1}$. Dynafit simulations published elsewhere show that these rates result in an electron originally residing in the b_H heme of one monomer to equilibrate with the other within 3 ms, equivalent to a net rate of $\sim 300\ s^{-1}$ [31].

3. Results

3.1 Reduction kinetics of cytochrome b and cytochrome c_1

The reduction of the isolated yeast bc_1 complex with decyl-ubiquinol in the presence of decyl-ubiquinone in a ratio of 1:3 is shown in Fig. 2. Cytochrome c_1 was reduced with biphasic kinetics with ~62% of the heme undergoing reduction in the first phase ($k = 5.6\ s^{-1}$) after a lag phase that lasted about 25 ms (Fig. 2, insert). In contrast, the reaction of cytochrome *b* with quinol and quinone was triphasic, with a prominent reduction phase almost four times faster than the early cytochrome c_1 reduction ($k = 21\ s^{-1}$). This fast reduction of cytochrome *b* had almost reached its maximum by 0.1 s, time point at which the first kinetic phase of cytochrome c_1 reduction had proceeded to only ~25% of its total extent. The completion of the first cytochrome c_1 kinetic phase was accompanied by a slight reoxidation of cytochrome *b*. The much slower reduction of the remaining cytochrome c_1 ($k \sim 0.1\ s^{-1}$) proceeded as cytochrome *b* was also slowly reduced back to approximately the same level as had originally been reached during the early fast reduction phase. The incomplete reduction of cytochrome c_1 in a single phase is probably due to the Rieske protein becoming almost fully reduced before c_1 by virtue of the higher E_m of the iron-sulfur cluster at neutral pH. This results in a much slower oxidation of quinol at center P because of the tendency of electrons to stay in the Rieske protein. The lag phase of cytochrome c_1 reduction is more enigmatic, but might reflect a hysteresis property of center P when the fully oxidized enzyme is exposed to quinol.

3.2 Cytochrome b reduction at different quinol and quinone concentrations

The triphasic cytochrome *b* reduction pattern was more fully characterized by varying the concentration of decyl-ubiquinol and decyl-ubiquinone in the assay. As shown in Fig. 3, at any fixed quinol concentration, an increase in quinone resulted in a decrease in the extent of the fast phase of cytochrome *b* reduction. Considering the extinction coefficient of the b_H heme ($36\ mM^{-1}\ cm^{-1}$) and a pathlength of 2 cm in the reaction chamber of the stopped flow spectrophotometer, the extent of fast reduction observed in the first kinetic phase varied from 33% to 55% of the b_H hemes depending on the quinol and quinone concentrations. The quinone-dependent loss of fast b_H reduction reflected a fast oxidation event different from the subsequent slower reoxidation event. When no decyl-ubiquinone was added, or at the highest concentrations of decyl-ubiquinol, the slow reoxidation phase was not observable (Figs. 3A–D). It was more evident at intermediate quinone concentrations (7.5 and 15 μM) at the lowest decyl-ubiquinol concentration used (Fig. 3A), but its extent decreased again as the further addition of quinone resulted in a faster initial oxidation of the b_H hemes. The final kinetic phase, consisting of a slow additional reduction, was present in all conditions, although its extent increased at higher quinol/quinone ratios.

3.3 Kinetic differences between cytochrome b and c_1 reduction

Although the extent of fast cytochrome *b* reduction varied ~50% over the range of decyl-ubiquinone concentrations used, its rate showed relatively little change, as shown in Fig. 4A. The fitting of the initial rates of b_H reduction to a simple inhibition function yielded inhibition constants (K_i) for decyl-ubiquinone of 150–200 μM. In contrast, fitting the rates as a function of decyl-ubiquinol to the Michaelis-Menten equation yielded K_m values of ~40 μM (fitting not shown). This indicates that the site of the fast initial cytochrome *b* reduction has a significantly higher affinity for quinol than for quinone in when the enzyme is in the fully oxidized state at which the reaction was started.

Cytochrome c_1 reduction, which is the result of center P catalysis, displayed an opposite affinity pattern toward quinone and quinol. As shown in Fig. 4B, a 50% decrease in the rate of the initial reduction was observed at 45 μM of decyl-ubiquinone, which is the K_i value obtained from the fitted inhibition curves. This value is 4–5 times lower than the one calculated from

cytochrome *b* reduction rates (see Fig. 4A). In contrast, the dependency of the c_1 reduction rates on decyl-ubiquinol concentration was linear in the range used, implying that the K_m value is several times higher than the highest concentration used, which was 30 μM. Therefore, it becomes evident that the initial reduction of cytochrome *b* and of cytochrome c_1 occur at different sites in the enzyme. This agrees with the higher rates for b_H reduction than for cytochrome c_1 at each individual quinol and quinone combination (compare Figs. 4A and B). Moreover, the difference in the reduction rates of the two cytochromes was not constant, but varied between a 2-fold faster reduction of cytochrome *b* (for example, at 30 μM decyl-ubiquinol and no decyl-ubiquinone) and a factor of 4 (at 15 μM of quinol substrate and without added quinone). This leads to the conclusion that the faster reduction of cytochrome *b* occurs by direct equilibration of the quinone pool through center N.

3.4 Insensitivity of center P catalysis to b_H pre-reduction through center N

The partial reduction of the b_H hemes through center N that precedes center P catalysis is shown in Fig. 5A at selected quinol/quinone ratios corresponding in all cases to a total of 30 equivalents of decyl-ubiquinol + decyl-ubiquinone per bc_1 monomer. Slightly less than 1 equivalent of endogenous ubiquinone copurified with the enzyme was also present. It was only at the highest ratio that the initial cytochrome *b* reduction surpassed the level corresponding to 50% of the b_H hemes. Surprisingly, it was only at this high quinol/quinone ratio that a modest decrease of 10% in the extent of initial cytochrome c_1 reduction was observed, as shown in Fig. 5B. This implies that an average reduction of up to one b_H heme per monomer did not have any discernible effect in the number of bc_1 monomers that were able to oxidize quinol in spite of the unavailability of a significant proportion of the b_H hemes to accept one of the electrons from center P catalysis. Fig. 5 also evidences the higher sensitivity of center P rates to variations in quinol/quinone ratios relative to center N. Furthermore, the kinetic traces show that the slow and slight reoxidation of the b_H hemes observed at the lowest ratios (or the slower further reduction at the highest ratios) occurred at the same time as center P catalysis was proceeding, implying a re-equilibration through center N as the electrons from quinol oxidation at center P arrive.

The possible role of the dimeric structure of the bc_1 complex in the lack of center P inhibition in the face of partial b_H pre-reduction were investigated by simulating the electron distribution in the b_H hemes upon equilibration of quinol and quinone through center N. As shown in Fig. 6 using a dimeric model, the movement of electrons from one monomer to the other after reduction of the b_H heme with quinol generates certain dimer states that would allow unimpeded center P catalysis, such as dimers with oxidized b_H heme and semiquinone at both center N sites. This species constituted 20%, 15% and 9% of the total population of dimers in the simulations of quinol/quinone ratios of 0.33, 1, and 3, respectively (Fig. 6A–C, dashed trace). Only at the highest ratio of >30 did the concentration of this doubly oxidized dimer with semiquinone drop below 1% (Fig. 6D, dashed trace). The most abundant enzyme conformation found in the simulations using a dimeric model was that of bc_1 complexes with one b_H heme reduced and the other oxidized with semiquinone at one of the center N sites (solid curves in Fig. 6). Its concentration was estimated to be of 25–37% of the total dimer population at all four quinol/quinone ratios simulated, even spiking to 40% within the first 10 ms at the highest ratio of >30 before slowly decreasing during the next 20 ms (Fig. 6D), favoring center P catalysis during this time range. This species is in reality a mixture of conformations in which the electron can reside in the b_H heme at a vacant or at a semiquinone-bound center N. Nevertheless, equilibration between the monomers would allow electrons coming from center P quinol oxidation to reach the oxidized b_H heme. Potentially inhibitory conformations for center P in which both b_H hemes are pre-reduced (with or without semiquinone bound) stayed below a concentration of 20% up to a quinol/quinone ratio of 3 before more than doubling to 46% at the highest ratio of >30 (dashed-dotted lines in Fig. 6). However, even in this condition

the concentration of this fully reduced b_H dimer remained under 30% before 30 ms, when the first kinetic phase of quinol oxidation at center P is expected to be halfway complete (compare Fig. 6C with 5B).

When center N equilibration was simulated assuming no electron communication between monomers, the only reduced species that could be formed was that of a semiquinone-bound center N site with the b_H heme reduced. In the monomeric model, this conformation is expected to be detrimental to center P catalysis, since it would allow only the low potential b_L heme to be available as acceptor for one of the electrons form quinol oxidation, with no possibility of the electron going to the other b_H heme in the dimer. The concentration of this species was calculated to be 23% even at the lowest quinol/quinone ratio of 0.33 (Fig. 6A dotted curve), and then increased from 36% to 46% between the ratios of 1 and >30 (Figs. 6B–D, dotted traces). Therefore, this monomeric model could not explain the constancy in the number of active center P sites at the various quinol/quinone ratios.

4. Discussion

The first main conclusion of the present work is that the first kinetic component of the triphasic reduction of cytochrome *b* in the uninhibited bc_1 complex is the result of a fast equilibration of the b_H hemes with quinol and quinone directly through center N, without significant influence from the slower center P catalysis. We have recently argued this to be the case [27, 32], although in the past it was considered that this initial reduction reflected the arrival of an electron from the first turnover at center P [11,12,19,20]. This interpretation was based on the observations that the rates of cytochrome c_1 and cytochrome *b* were similar in a succinate-cytochrome *c* oxidoreductase assay [11], or in the isolated bc_1 complex upon reduction with menadiol [12]. Addition of center P inhibitors resulted in a mild [11] or significant [12] decrease in the rate of initial cytochrome *b* reduction, suggesting that center P was responsible for its early reduction. However, it had been shown earlier using submitochondrial particles or the succinate-cytochrome c oxidoreductase preparation that the initial rate of cytochrome *b* reduction by duroquinol in the absence of inhibitors was much faster than that in the presence of antimycin [33], and was very fast even in the presence of myxothiazol [34]. Experiments with bacterial chromatophores have not contributed to clarifying this issue, since the bc_1 complex and the quinone pool are pre-equilibrated with redox mediators before the reaction is started, resulting in very little additional reduction of the b_H hemes in the absence of inhibitors [17]. Using more physiological ubiquinol analogs, it has more recently been shown that reduction of the isolated uninhibited enzyme results in a several-fold faster initial reduction of cytochrome *b* with respect to c_1 [19], as we presently report (see Fig. 2). The thinking that this faster *b* reduction comes from center P has led to the proposals that the movement of the Rieske protein toward cytochrome c_1 is the rate-limiting step of the enzyme [35], that antimycin slows down the intrinsic rate of center P catalysis [19], or even that b_L to b_H electron transfer is not the electrogenic step in the Q cycle [20], all of which have been disproved experimentally [16,36,37].

We have now shown that the early reduction of cytochrome *b*, besides being faster and starting earlier than c_1 reduction (see Fig. 2), exhibits an apparently instantaneous partial oxidation that decreases its initial extent as decyl-ubiquinone concentration is increased (see Fig. 3). However, its rate is very weakly influenced by quinone, in contrast to what is observed at center P (see Fig. 4). These kinetic features of the fast initial b_H reduction are the same as we have reported when center N is studied in the presence of center P inhibitors [15], and can be explained by assuming a redox-specific binding of quinol and quinone depending on the redox state of the b_H heme at each center N, together with electron crossover between cytochrome *b* subunits [13,15]. This implies that center N equilibrates rapidly with the quinone pool before center P catalysis proceeds, as has been incorporated in certain mechanisms, which propose

the "priming" of the enzyme previous to quinol oxidation [38]. The lag phase we now report in cytochrome c_1 that lasts almost up to the completion of the initial *b* reduction phase (see Fig. 2) would be consistent with such a model. Further proof that the initial rate of cytochrome *b* reduction in the absence of inhibitors corresponds to a reaction through center N is its insensitivity to the Y185F mutation in the Rieske protein that lowers the redox potential of the iron-sulfur cluster (data not shown) or to the E272Q mutation in cytochrome *b* [32]. In contrast, we have already reported that cytochrome *b* reduction in the presence of antimycin (which can only occur through center P) was markedly lowered by both of these mutations [32,37].

The second phase observed in cytochrome *b* kinetics, consisting of a slight reoxidation observed at low quinol/quinone ratios, occurred as cytochrome c_1 reduction was proceeding. As has been discussed previously [11,12], this implies that the electrons being transferred to center N from quinol oxidation at center P favor b_H oxidation, probably by consuming the semiquinone previously formed at center N by reduction of the b_H heme by quinol. When quinone is sufficiently high relative to quinol, it can bind again to center N to form more semiquinone, consuming the electrons that reach the b_H heme from center P. Once center P catalysis can no longer proceed upon full reduction of the Rieske protein, quinol can again reduce the b_H hemes, resulting in the third and last phase consisting of a re-reduction of the b_H hemes.

The second main conclusion from the present studies is that the electron communication between cytochrome *b* subunits in the dimer allows center P catalysis to proceed uninhibited by the earlier reduction of some of the b_H hemes. In the presence of a pre-reduced b_H heme, the equilibrium constant for quinol oxidation at center P is close to 1 [17], implying that turnover at center P sites would stop at quinol/quinone ratios ≤1. Even when quinol is in excess with respect to quinone (favoring the $K_{eq} = 1$ reaction), we have found that center P catalysis does not proceed when the b_H hemes are fully reduced after two turnovers in the center N-inhibited yeast enzyme dimer [37]. This probably is due to a higher affinity of center P toward quinone than quinol (see Fig. 4B), some electrostatic effect that makes b_L reduction less favorable when the b_H heme is reduced [39], or leakage of electrons from cytochrome *b* to oxygen that prevents electrons from accumulating in the b_L heme. In any event, the pre-reduction of ~50% of the b_H hemes should be expected to decrease significantly the number of center P sites that are able to oxidize quinol. However, it was only at the highest quinol concentration assayed (without exogenous quinone added) that a slight decrease in the number of active center P sites (~10%) was observed (see Fig. 5B). Since at this extreme quinol/quinone ratio a b_H pre-reduction level of 50% was surpassed (see Fig. 5A), center P catalysis at a few dimers in the enzyme population likely became inhibited because of having both b_H hemes already in a reduced state by rapid equilibration through center N.

The simulations we now present (see Fig. 6) underscore the importance of the dimeric structure in allowing electron equilibration between monomers, thereby maximizing the availability of oxidized acceptors for one of the electrons coming from each quinol oxidation event at center P [13,15]. The relevance of b_L to b_L electron transfer has been proposed to be especially important when some reduction of the b_H hemes has occurred [29,40], as we illustrate in Fig. 7. In this model, some of the possible conformations of the dimer that can be formed upon fast equilibration of electrons through center N prior to center P catalysis. The initially oxidized dimer binds quinol at one of its center N sites resulting in formation of semiquinone and reduction of the adjacent b_H heme (intermediate I). Two possible reactions can follow. First, the electron could equilibrate to the other monomer, reducing the b_H heme at the second center N site, followed by quinone binding and reduction to form semiquinone (II). Alternatively, another quinol molecule could bind to the second center N site to reduce its b_H heme (II′). Both of these intermediates have two semiquinones, but only the species with the two b_H hemes in the oxidized state would be poised for optimal catalysis at center P. The concentration of this

fully oxidized species is expected to be significant at quinol/quinone ratios ≤ 1 (see Fig. 6A and B), which corresponds to the physiological range of 0.1–0.7 reported in respiring mitochondria [41].

Semiquinone is a tightly bound species [8–10], but it can be assumed to be in fast equilibrium with the b_H heme, rapidly changing to quinol or quinone. If in the fully oxidized intermediate (II in Fig. 7) one semiquinone donates its electron to the adjacent b_H heme, a species with one semiquinone and one oxidized b_H heme would be formed (intermediate III). A similar conformation would be reached when one of the two semiquinones in the intermediate with both b_H hemes reduced (II′) accepts an electron to form quinol (III′), except that this intermediate would initially have the remaining semiquinone next to the reduced heme. However, equilibration of the electron via the b_L hemes would allow continuous inter-conversion between intermediates III and III′. Our simulations suggest that between 25% and 36% of the dimer population exists in one of these two conformations at all quinol/quinone ratios (see Fig. 6).

There are other possible equilibration reactions that could occur from these two intermediates that lead to conformations not depicted in Fig. 7, but that were included in the simulations of Fig. 6. For example, the single semiquinone in intermediate III could reduce the b_H heme upon conversion to quinone and leave the dimer with two reduced b_H hemes in the two empty center N sites. This species, together with the reduced dimer with two semiquinones (intermediate II ′), is shown in the simulations of Fig. 6 as the sum of all dimers with two reduced b_H hemes. Alternatively, semiquinone could oxidize the reduced b_H heme in intermediate III′ to form quinol, resulting in a fully oxidized dimer with its two center N sites empty. This species is the same as the initial state of the enzyme before reaction with quinol, and was found to vary between 22% and 4% as the quinol/quinone ratio was increased from 0.33 to <30 (not shown). It is evident that quinol oxidation could proceed unimpeded from this fully oxidized intermediate, as well as from intermediate II. However, these two conformations in which both center N sites are in the same state would be able to catalyze quinol oxidation in only one monomer, as we have proposed in several studies that have evidenced a half-of-the-sites activity at center P [14,37].

The dimer conformations with one semiquinone and one reduced b_H heme (intermediates III and III′ in Fig. 7) would also allow center P catalysis. Quinol oxidation could occur in the same monomer in which the b_H heme is oxidized (intermediates IVa and IVb′), or even in the monomer where the b_H heme is reduced by transferring the electron via the b_L hemes to the opposite center N site where b_H is oxidized (IVb and IVa′). We have proposed that quinol oxidation can occur in both center P sites simultaneously when only one semiquinone is stabilized in the dimer (intermediates III and III′) [14,37]. However, the symmetry at the two center N sites would be quickly regained upon quinol oxidation at any of the two active center P sites, either by consuming the only semiquinone (IVa and IVb) both center N sites, or by forming a second semiquinone (IVa′ and IVb′). Thus, a subsequent quinol oxidation event from any of these symmetrical center N dimers conformations would occur at only one center P site, with the other being inactive again.

Our present results support the notion that the dimeric structure of the bc_1 complex has been selected to allow maximal activity of the two quinol/quinone oxido-reduction sites (center P and center N), circumventing the potential risks of having two catalytic sites functioning in opposite direction to each other. Therefore, an adequate understanding of the Q cycle mechanism of energy conservation that operates in the cytochrome bc_1 complex should include a description of the reactions and electron transfers that occur in the context of the dimeric arrangement of this enzyme.

References

1. Zhang ZL, Huang LS, Shulmeister VM, Chi YI, Kim KK, Hung LW, Crofts AR, Berry EA, Kim SH. Electron transfer by domain movement in cytochrome bc_1. Nature 1998;392:677–684. [PubMed: 9565029]
2. Yu CA, Xia D, Kim H, Deisenhofer J, Zhang L, Kachurin AM, Yu L. Structural basis of functions of the mitochondrial bc_1 complex. Biochim Biophys Acta 1998;1365:151–158. [PubMed: 9693733]
3. Iwata S, Lee JW, Okada K, Lee JK, Iwata M, Rasmussen B, Link TA, Ramaswamy S, Jap BK. Complete structure of the 11-subunit bovine mitochondrial cytochrome bc_1 complex. Science 1998;281:64–71. [PubMed: 9651245]
4. Hunte C, Koepke J, Lange C, Rossmanith T, Michel H. Structure at 2.3 Å resolution of the cytochrome bc_1 complex from the yeast *Saccharomyces cerevisiae* co-crystallized with an antibody Fv fragment. Structure 2000;8:669–684. [PubMed: 10873857]
5. Berry EA, Huang LS, Saechao LK, Pon NG, Valkova-Valchanova M, Daldal F. X-Ray Structure of *Rhodobacter capsulatus* cytochrome bc_1: Comparison with its mitochondrial and chloroplast counterparts. Photosynth Res 2004;81:251–275. [PubMed: 16034531]
6. Mitchell P. Possible molecular mechanisms of the protonmotive function of cytochrome systems. J Theor Biol 1976;62:327–367. [PubMed: 186667]
7. Brandt U, Trumpower B. The protonmotive Q cycle in mitochondria and bacteria. Crit Rev Biochem Mol Biol 1994;29:165–197. [PubMed: 8070276]
8. Ohnishi T, Trumpower BL. Differential effects of antimycin on ubisemiquinone bound in different environments in isolated succinate-cytochrome c reductase complex. J Biol Chem 1980;255:3278–3274. [PubMed: 6245075]
9. De Vries S, Berden JA, Slater EC. Properties of a semiquinone anion located in the QH_2:cytochrome c oxidoreductase segment of the mitochondrial respiratory chain. FEBS Lett 1980;122:143–148. [PubMed: 7215541]
10. Robertson DE, Prince RC, Bowyer JR, Matsuura K, Dutton PL, Ohnishi T. Thermodynamic properties of the semiquinone and its binding site in the ubiquinol-cytochrome c (c_2) oxidoreductase of respiratory and photosynthetic systems. J Biol Chem 1984;259:1758–1763. [PubMed: 6319410]
11. Tang H, Trumpower BL. Triphasic reduction of cytochrome *b* and the protonmotive Q cycle pathway of electron transfer in the cytochrome bc_1 complex of the mitochondrial respiratory chain. J Biol Chem 1986;261:6209–6215. [PubMed: 3009448]
12. Snyder CH, Trumpower BL. Ubiquinone is responsible for triphasic reduction of cytochrome *b* in the cytochrome bc_1 complex. J Biol Chem 1999;274:31209–31216. [PubMed: 10531315]
13. Covian R, Trumpower BL. Rapid electron transfer between monomers when the cytochrome bc_1 complex dimer is reduced through center N. J Biol Chem 2005;280:22732–22740. [PubMed: 15833742]
14. Covian R, Trumpower BL. Regulatory interactions between ubiquinol oxidation and ubiquinone reduction sites in the dimeric cytochrome bc_1 complex. J Biol Chem 2006;281:30925–30932. [PubMed: 16908520]
15. Covian R, Zwicker K, Rotsaert FA, Trumpower BL. Asymmetric and redox-specific binding of quinone and quinol at center N of the dimeric yeast cytochrome bc_1 complex. Consequences for semiquinone stabilization. J Biol Chem 2007;282:24198–24208. [PubMed: 17584742]
16. Osyczka A, Moser CC, Daldal F, Dutton PL. Reversible redox energy coupling in electron transfer chains. Nature 2004;427:607–612. [PubMed: 14961113]
17. Crofts AR, Shinkarev VP, Kolling DR, Hong S. The modified Q-cycle explains the apparent mismatch between the kinetics of reduction of cytochromes c_1 and b_H in the bc_1 complex. J Biol Chem 2003;278:36191–36201. [PubMed: 12829696]
18. Kramer DM, Roberts AG, Muller F, Cape J, Bowman MK. Q-cycle bypass reactions at the Qo site of the cytochrome bc_1 (and related) complexes. Methods Enzymol 2004;382:21–45. [PubMed: 15047094]
19. Hansen KC, Schultz BE, Wang G, Chan SI. Reaction of *Escherichia coli* cytochrome bo_3 and mitochondrial cytochrome bc_1 with a photoreleasable decylubiquinol. Biochim Biophys Acta 2000;1456:121–137. [PubMed: 10627300]

20. Klishin SS, Junge W, Mulkidjanian AY. Flash-induced turnover of the cytochrome bc_1 complex in chromatophores of *Rhodobacter capsulatus*: binding of Zn^{2+} decelerates likewise the oxidation of cytochrome *b*, the reduction of cytochrome c_1 and the voltage generation. Biochim Biophys Acta 2002;1553:177–182. [PubMed: 11997126]
21. Trumpower BL, Edwards CA. Purification of a reconstitutively active iron-sulfur protein (oxidation factor) from succinate : cytochrome c reductase complex of bovine heart mitochondria. J Biol Chem 1979;254:8697–8706. [PubMed: 224062]
22. Rich PR. Electron and proton transfers through quinones and cytochrome bc complexes. Biochim Biophys Acta 1984;768:53–79. [PubMed: 6322844]
23. Ljungdahl PO, Pennoyer JD, Robertson DE, Trumpower BL. Purification of highly active cytochrome bc_1 complexes from phylogenetically diverse species by a single chromatographic procedure. Biochim Biophys Acta 1987;891:227–241. [PubMed: 3032252]
24. Snyder C, Trumpower BL. Mechanism of ubiquinol oxidation by the cytochrome bc_1 complex: pre-steady-state kinetics of cytochrome bc_1 complexes containing site-directed mutants of the Rieske iron-sulfur protein. Biochim Biophys Acta 1998;1365:125–134. [PubMed: 9693731]
25. Yu CA, Yu L, King TE. Preparation and properties of cardiac cytochrome c1. J Biol Chem 1972;247:1012–1019. [PubMed: 5010060]
26. Berden JA, Slater EC. The reaction of antimycin with a cytochrome b preparation active in reconstitution of the respiratory chain. Biochim Biophys Acta 1970;216:237–249. [PubMed: 5504626]
27. Rotsaert FAJ, Covian R, Trumpower BL. Mutations in cytochrome *b* that affect kinetics of the electron transfer reactions at center N in the yeast cytochrome bc_1 complex. Biochim Biophys Acta 2008;1777:239–249. [PubMed: 18328328]
28. Kuzmic P. Program DYNAFIT for the analysis of enzyme kinetic data: application to HIV proteinase. Anal Biochem 1996;237:260–273. [PubMed: 8660575]
29. Moser CC, Farid TA, Chobot SE, Dutton PL. Electron tunneling chains of mitochondria. Biochim Biophys Acta 2006;1757:1096–1109. [PubMed: 16780790]
30. Crofts AR, Rose S. Marcus treatment of endergonic reactions: a commentary. Biochim Biophys Acta 2002;1767:1228–1232. [PubMed: 17720135]
31. Covian R, Trumpower BL. Regulatory interactions in the dimeric cytochrome bc_1 complex: The advantages of being a twin. Biochim Biophys Acta. 2008in press
32. Wenz T, Covian R, Hellwig P, Macmillan F, Meunier B, Trumpower BL, Hunte C. Mutational analysis of cytochrome *b* at the ubiquinol oxidation site of yeast complex III. J Biol Chem 2007;282:3977–3988. [PubMed: 17145759]
33. De Vries S, Albracht SP, Berden JA, Slater EC. The pathway of electrons through QH_2:cytochrome c oxidoreductase studied by pre-steady-state kinetics. Biochim Biophys Acta 1982;681:41–53. [PubMed: 6288082]
34. De Vries S, Albracht SP, Berden JA, Marres CA, Slater EC. The effect of pH, ubiquinone depletion and myxothiazol on the reduction kinetics of the prosthetic groups of ubiquinol:cytochrome *c* oxidoreductase. Biochim Biophys Acta 1983;723:91–103. [PubMed: 6299337]
35. Yu CA, Wen X, Xiao K, Yu L. Inter- and intra-molecular electron transfer in the cytochrome bc1 complex. Biochim Biophys Acta 2002;1555:65–70. [PubMed: 12206893]
36. Crofts AR, Hong S, Zhang Z, Berry EA. Physicochemical aspects of the movement of the Rieske iron-sulfur protein during quinol oxidation by the bc_1 complex from mitochondria and photosynthetic bacteria. Biochemistry 1999;38:15827–15839. [PubMed: 10625447]
37. Covian R, Gutierrez-Cirlos EB, Trumpower BL. Anti-cooperative oxidation of ubiquinol by the yeast cytochrome bc_1 complex. J Biol Chem 2004;279:15040–15049. [PubMed: 14761953]
38. Mulkidjanian AY. Proton translocation by the cytochrome bc_1 complexes of phototrophic bacteria: introducing the activated Q-cycle. Photochem Photobiol Sci 2007;6:19–34. [PubMed: 17200733]
39. Shinkarev VP, Crofts AR, Wraight CA. The electric field generated by photosynthetic reaction center induces rapid reversed electron transfer in the bc_1 complex. Biochemistry 2001;40:12584–12590. [PubMed: 11601982]

40. Shinkarev VP, Wraight CA. Intermonomer electron transfer in the bc_1 complex dimer is controlled by the energized state and by impaired electron transfer between low and high potential hemes. FEBS Lett 2007;581:1535–1541. [PubMed: 17399709]

41. Klingenberg, M.; Kroger, A. On the role of ubiquinone in the respiratory chain. In: Slater, EC.; Kaniuga, Z.; Wojtczak, L., editors. Biochemistry of Mitochondria. Academic Press; New York: 1967. p. 11-27.

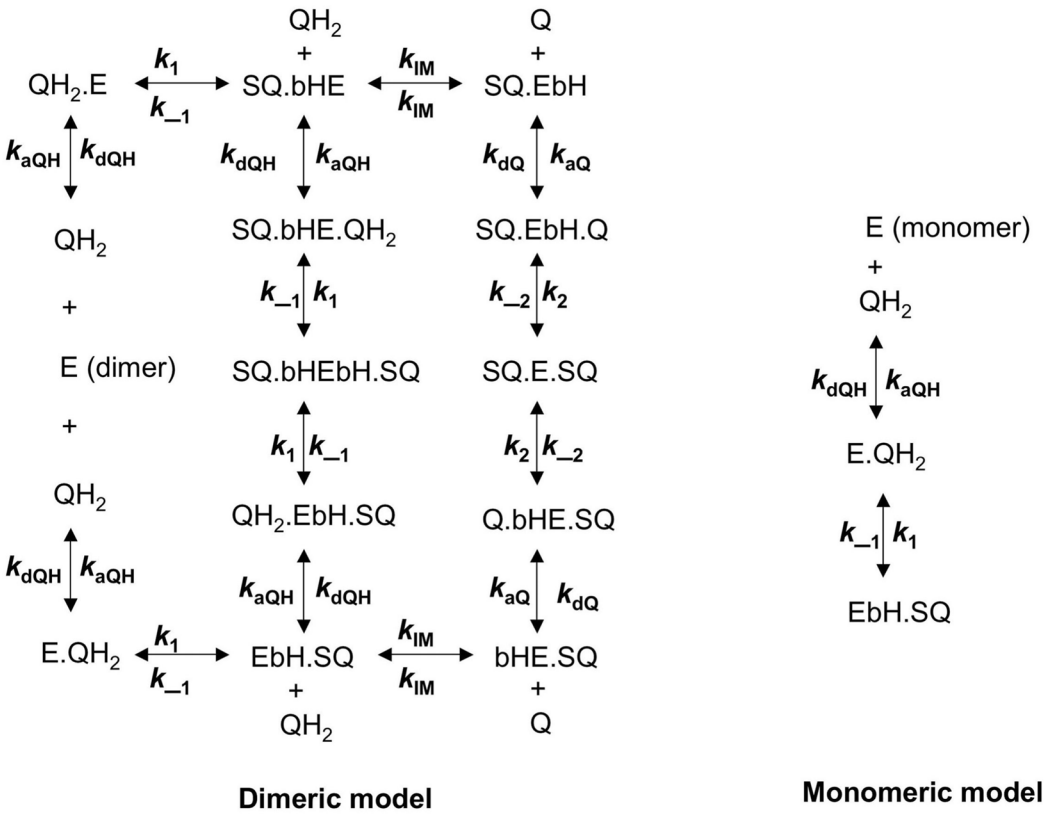

Fig. 1. Models used for the kinetic simulation of electron equilibration through center N

The dimeric model (left) assumed that electrons could equilibrate between the b_H hemes in each monomer with a rate defined as k_{IM}. For clarity, not all the possible reactions between species are shown, but were included in the simulations The monomeric model (right) considered each center N site as isolated from the other monomer, with electron equilibration occurring only between the b_H heme and quinol (QH_2) or semiquinone (SQ). Kinetic constants refer to the association and dissociation rates for quinol (k_{aQH}, k_{dQH}), and quinone (k_{aQ}, k_{dQ}), as well as to the forward and reverse rates of conversion of quinol to semiquinone (k_1 and k_{-1}) and of semiquinone to quinone (k_2 and k_{-2}). The values assigned to each constant are explained under “Materials and methods”.

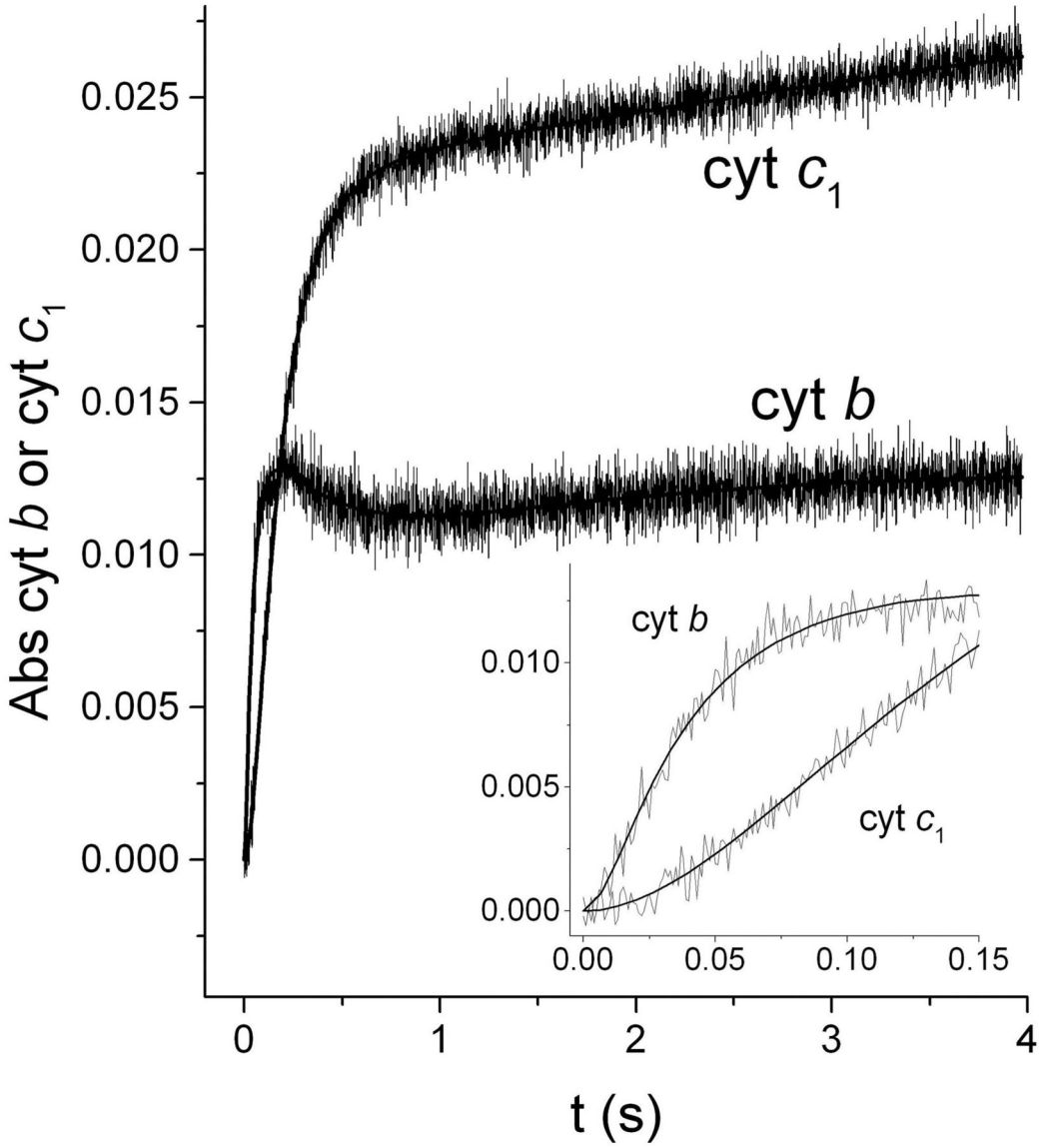

Fig. 2. Pre-steady state reduction of cytochrome *b* and cytochrome c_1 in the yeast cytochrome bc_1 complex

Traces show the reduction kinetics of 1 μM yeast bc_1 complex 7.5 μM decyl-ubiquinol in the presence of 22.5 μM decyl-ubiquinone measured at 562–578 nm (cytochrome *b*) and 554–539 nm (cytochrome c_1, corrected for the spectral contribution of cytochrome *b* as explained in Ref. 34). The solid curves correspond to the best fit to a third order (*b*) or second order (c_1) exponential function. Fitted values for cytochrome *b* were $k_1 = 21 \pm 0.7\ s^{-1}$ (Abs 0.015 ± 0.0004), $k_2 = 2.5 \pm 0.4\ s^{-1}$ (Abs −0.007 ± 0.001), $k_3 = 0.8 \pm 0.2$ (Abs 0.004 ± 0.001). For cytochrome c1, the fitted values were $k_1 = 5.6 \pm 0.06\ s^{-1}$ (Abs 0.022 ± 0.0001), $k_2 = 0.9 \pm 0.02\ s^{-1}$ (Abs 0.013 ± 0.003).

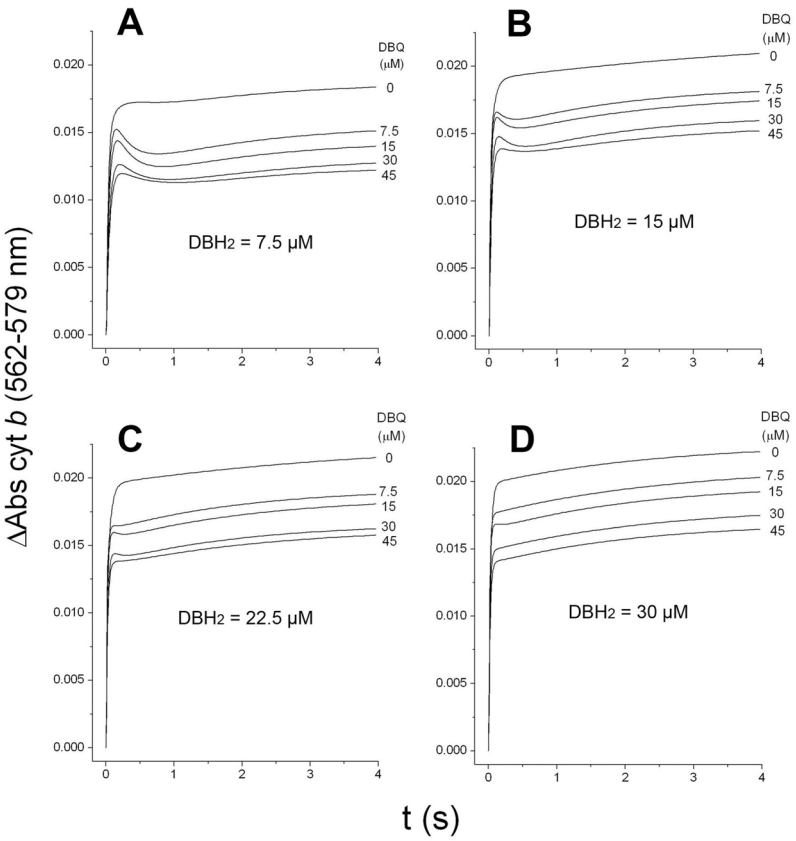

Fig. 3. Pre-steady state reduction of cytochrome *b* as a function of quinol and quinone concentration

Cytochrome *b* reduction traces were obtained by reducing 1 μM yeast bc_1 complex with the indicated concentrations of decyl-ubiquinol (DBH_2) in the presence of varying decyl-ubiquinone (DBQ) concentrations. The experimental data points were then fitted to a second or third order exponential function. For clarity, the experimental traces have been removed to show only the fitted curves.

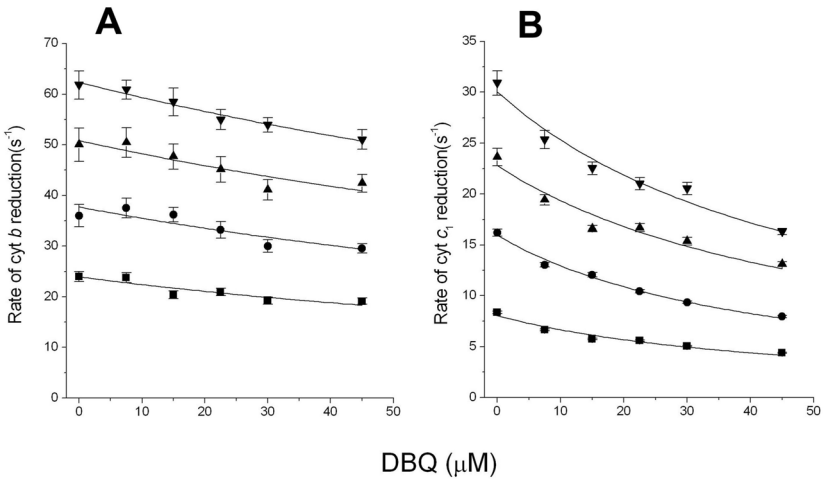

Fig. 4. Initial rates of cytochrome *b* and cytochrome c_1 reduction at different quinol and quinone concentrations

The rates obtained for the first kinetic phase of cytochrome *b* (panel A) and cytochrome c_1 (panel B) reduction by 7.5 μM (squares), 15 μM (circles), 22.5 μM (up triangles), and 30 μM (down triangles) of decyl-ubiquinol in the presence of different decyl-ubiquinone (DBQ) concentrations were fitted to a simple inhibition function. The K_i values for decyl-ubiquinone obtained from fitting the rates of cytochrome *b* reduction (A) were in the range of 150–200 μM, while those obtained for the rates of cytochrome c_1 reduction (B) were all close to 45 μM.

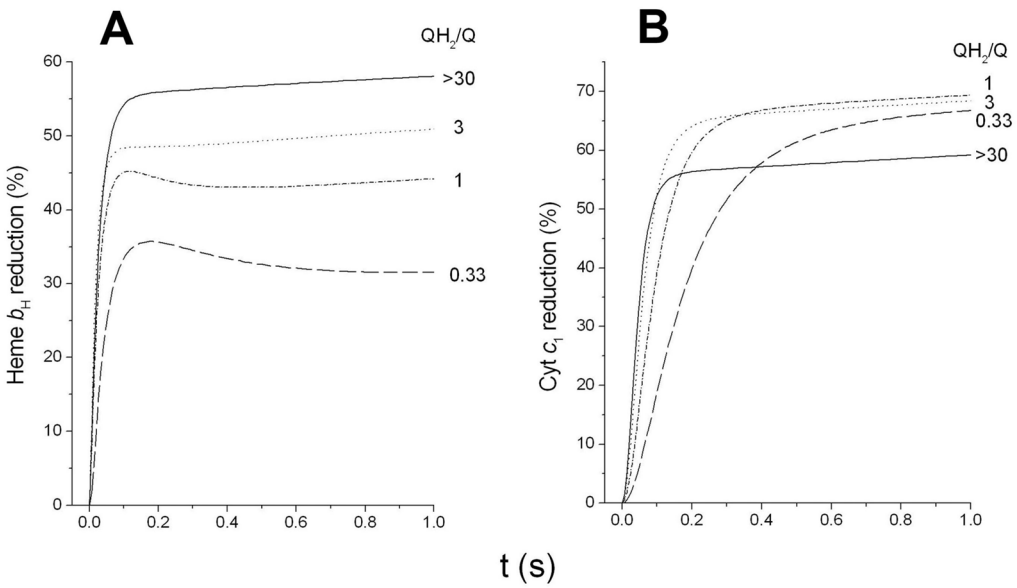

Fig. 5. Pre-steady state reduction of the yeast cytochrome bc_1 complex at different quinol/quinone ratios

The best-fit curves obtained from the experimental traces of cytochrome *b* and cytochrome c_1 reduction were plotted as a function of the proportion of b_H (panel A) and c_1 (panel B) hemes reduced using their corresponding extinction coefficients. The sum of decyl-ubiquinol and decyl-ubiquinone was maintained at a fixed concentration of 30 μM in all cases. The quinol/quinone ratio of >30 corresponds to 30 μM decyl-ubiquinol with no decyl-ubiquinone added. The only quinone present in this case was the ~0.9 μM of endogenous ubiquinone copurified with the enzyme.

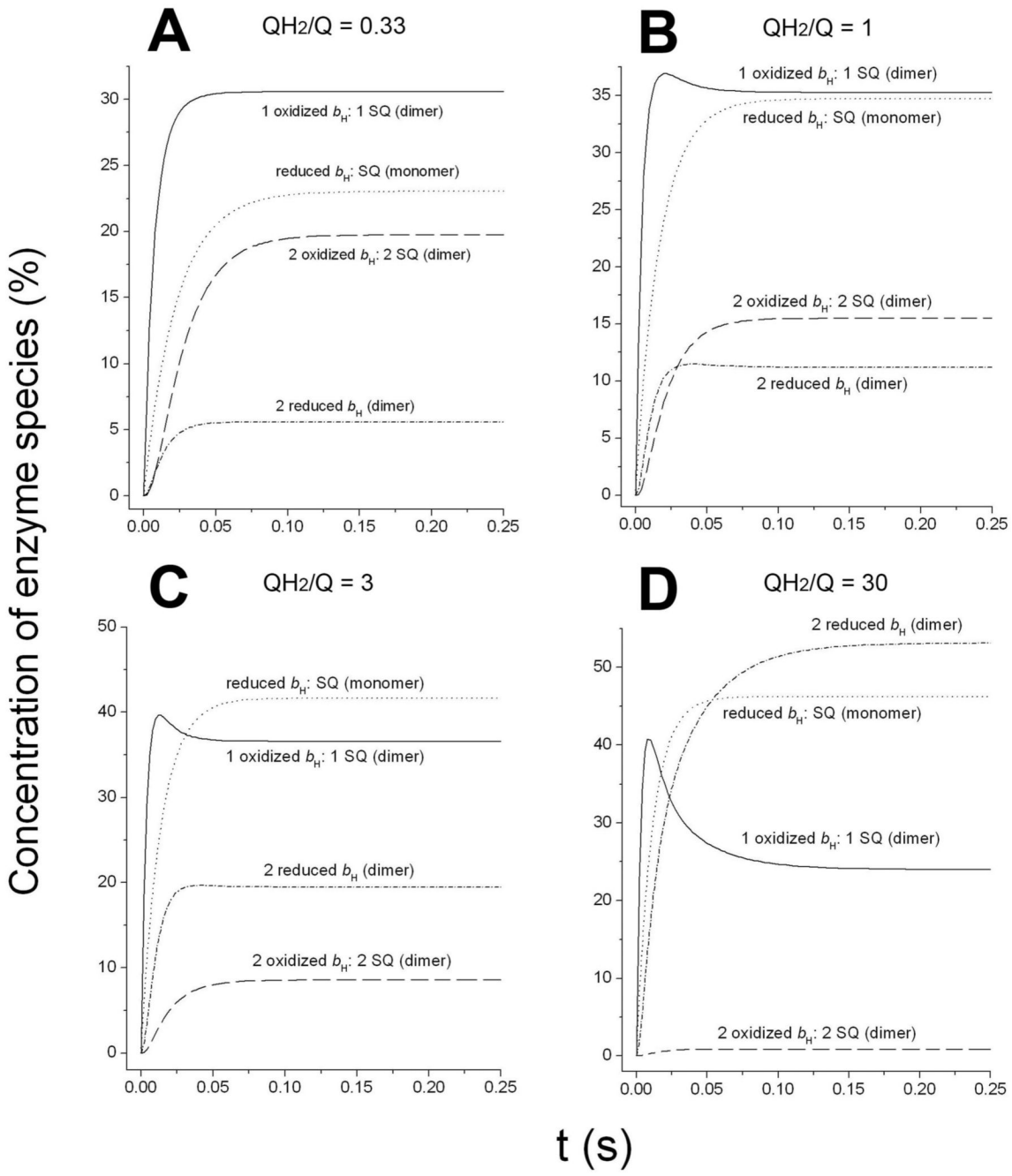

Fig. 6. Simulations of electron equilibration through center N at different quinol/quinone ratios

The models shown in Fig. 1 were used in the Dynafit program to simulate the kinetics of formation of different enzyme species upon equilibration of the quinol and quinone at the indicated ratios with the b_H hemes through center N. The species labeled as "dimer" were obtained using a dimeric model that assumes electron equilibration between the two b_H hemes. The species labeled "monomer" was calculated by assuming that no electron crossover in the dimer is possible. Details on the models are provided under "Materials and methods".

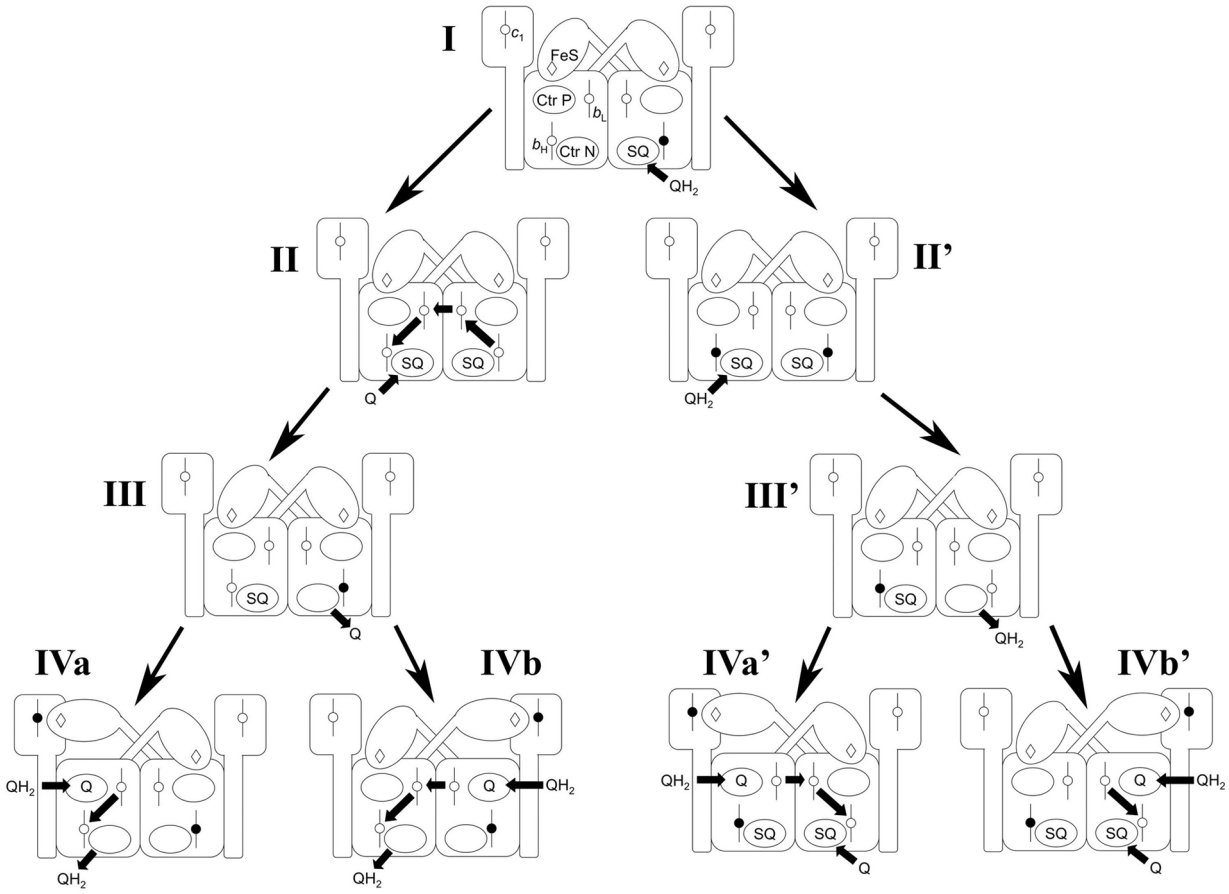

Fig. 7. Electron equilibration in the bc_1 complex dimer

Some of the possible conformations of the dimer formed upon equilibration of electrons through center N (intermediates I-III and I-III′) before catalysis at center P occurs (intermediates IVa, IVb, IVa′, and IVb′) are shown. As more fully explained under "Discussion", electron crossover between monomers via the b_L hemes (as shown in the formation of intermediates II, IVb and IVa′) allows quinol oxidation at center P even at dimers where one b_H heme has been pre-reduced through center N.